EFFICIENCY OF GASEOUS SHIELD ON ROUGH SURFACE

V. P. Komarov, A. I. Leont'ev,
L. A. Okolito, and V. G. Puzach

UDC 532.526.4

Results of a study are reported pertaining to the efficiency of a gaseous shield produced by injection of a gas through a permeable segment of a rough surface.

A great deal has been published in the technical literature on studies pertaining to the efficiency of gaseous shields variously produced on smooth surfaces [1-5]. Much less research has been done pertaining to the efficiency of a gaseous shield on a rough surface [6, 7]. Real surfaces are often rough because of structural characteristics or technological treatment and, therefore, there is a need for studying the effect of these forms of roughness on the efficiency of a gaseous shield and on the heat transfer in the region it covers.

For the efficiency of a gaseous shield produced by injection of gas through a predisengaged rough-surface in a zero-gradient subsonic turbulent stream there has been derived [1] the relation

$$\theta = \frac{T_w - T_0}{T_{w1} - T_0} = \left[1 + 0.016\beta_{max}\frac{Re_L\int_{\bar{x}_1}^{\bar{x}}\psi d\bar{x}}{Re_w^{1.25}(1+K_1)^{1.25}}\right]^{-0.8}, \qquad (1)$$

where $\beta_{max} = \frac{\delta}{\delta^{**}} - \frac{\delta^*}{\delta^{**}}$ and ψ represent the dimensionless law of friction within the shielded segment. Relation (1) is applicable to a rough surface as well as to a smooth surface when put in this form, inasmuch as it has been derived from the laws of energy and momentum conservation in the boundary layer.

For a smooth surface, with $\psi = 1$, we have $\beta_{max} = 9$ and expression (1) becomes [1]

$$\theta = \left[1 + 0.25\frac{Re_{\Delta x}}{Re_{w1}(1+K_1)^{1.25}}\right]^{-0.8} = [1 + 0.25R]^{-0.8}. \qquad (2)$$

For a rough surface, on the other hand, both β_{max} and the dimensionless law of friction depend on the dimensions and the spacing of asperities. They must be known and can, as a rule, be determined from experimental data on measured velocity profiles and friction laws in specific cases. Such data are available for various rough surfaces and can be used for determining ψ and β_{max}. Here we will generalize available data on drag and velocity profiles corresponding to square-law drag at rough surfaces. It is well known that drag obeys the square law above some critical Reynolds number Re_{cr2} which depends on the form and the distribution of the surface asperities as well as on the thickness of the boundary layer. We will assume that the numerical values of Re_{cr2} are known.

The graph in Fig. 1 depicts a generalization of experimental data on the drag of rough surfaces, in the form of the dimensionless friction law ψ_{rough} at a constant Re^{**}_{cr2} as a function of the relative asperity height, while the graph in Fig. 2 depicts a generalization of experimental data on the profiles of the dimensionless velocity ω in the boundary layer as a function of the coordinate y/δ^{**} at $Re^{**} \geq Re^{**}_{cr2}$. The experimental data used here include those according to [8, 9] on sandy roughness in pipes, data on a rectangular surface thread (S/K = 1.15) in a pipe [10], data on rectangular slats (S/K = 4) on a plate [11], data on rectangular grooves (S/K = 9) in a plate [12], data on a close-packed layer of balls on a plate [13], data on V-grooves (S/K = 0.5-4) in a pipe [14], data on threads (S/K = 0.34-1.52) in a pipe [15], and data from this study (hemispheres, S/K = 2-6, on a plate). The

Institute of High Temperatures, Academy of Sciences of the Ukrainian SSR, Moscow. Translated from Inzhenerno-Fizicheskii Zhurnal, Vol. 43, No. 6, pp. 885-891, December, 1982. Original article submitted November 2, 1981.

0022-0841/82/4306-1309$07.50

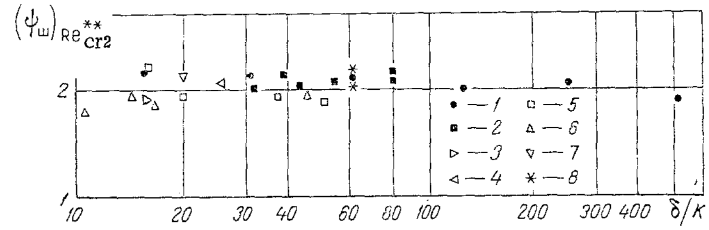

Fig. 1. Dimensionless law of friction at rough surfaces, at Re = Re_{cr2}: 1) Experimental data [8], 2) [13], 3) [12], 4) [10], 5) [14], 6) [15], 7) [11], 8) [9] (rectangular surface thread).

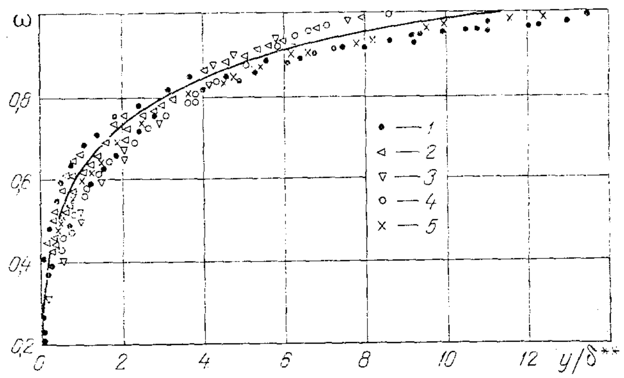

Fig. 2. Velocity profiles at rough surfaces, at Re ⩾ Re_{cr2}: 1) Experimental data [8], 2) [13], 3) [11], 4) this study, 5) [9].

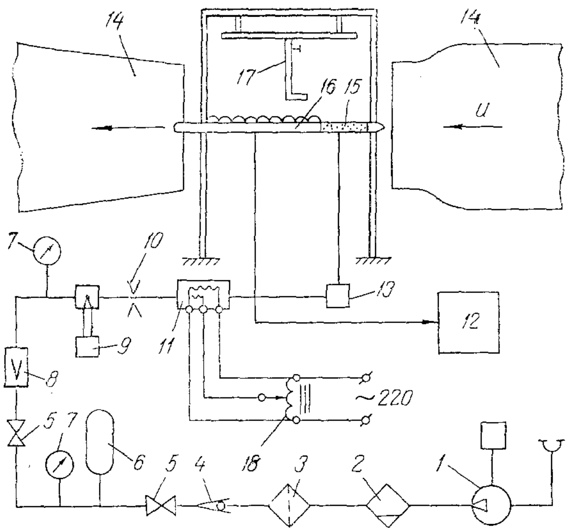

Fig. 3. Schematic diagram of experimental apparatus: 1) Electric compressor; 2) moisture separator; 3) filter; 4) check valve; 5) plain valve; 6) high-pressure tank; 7) manometer; 8) pressure reducer; 9) instrument for measuring air temperature; 10) normal diaphragm; 11) electric heater; 12) automatic temperature measuring system; 13) receptacle; 14) wind tunnel; 15) permeable segment; 16) insulated segment; 17) measuring probe; 18) autotransformer.

graph in Fig. 1 indicates that as the conditions of square-law drag are reached, the dimensionless law of friction at all rough surfaces under consideration here approaches the numerical value of 2:

$$\psi_{\text{rough}} = \left(\frac{c_f}{c_{f0}}\right)_{\text{Re}^{**}} = 2. \tag{3}$$

Relation (3) also remains valid when $\text{Re}^{**} \geqslant \text{Re}^{**}_{\text{cr}2}$, as before, and not to the actual value of the Reynolds number. It is to be noted in Fig. 2, that the profiles of dimensionless velocity above peaks of surface asperities can, in the case of square-law drag ($\text{Re}^{**} \geqslant \text{Re}^{**}_{\text{cr}2}$), be generalized with respect to the coordinate y/δ^{**} by the single relation

$$\omega = 0.5\,(3\omega_0^2 - \omega_0^4), \tag{4}$$

for all rough surfaces under consideration here, with ω_0 denoting the profile of dimensionless velocity above a smooth surface. The universality of such a dimensionless velocity profile with respect to the coordinate y/δ^{**} in the case of square-law drag was first noted by the authors of study [12]. Therefore, in the case of square-law drag of rough surfaces with various configurations of asperities (sand, balls, cylinders, threads, slats, grooves in walls) of relative dimensions within the $S/K = 0.34$–9 and R/K (or δ/K) = 10–600 range, one can use expressions (3) or (4) for calculating ψ_{rough} and $\beta_{\max}$. One must assume then that the critical Reynolds number $\text{Re}^{**}_{\text{cr}2}$ for a specific rough surface is known and that the velocity profile has been determined above the peaks of asperities.

With relation (4) taken into account, $\beta_{\max}$ for a rough plate streamlined under isothermal conditions will be

$$\beta_{\max} = \frac{\delta}{\delta^{**}} - \frac{\delta^{*}}{\delta^{**}} = \frac{1}{0.108} - \frac{0.152}{0.108} = 7.85. \tag{5}$$

Inserting values (3) and (5) into relation (1) yields, for the efficiency of a gaseous shield on a rough surface, the expression

$$\theta_{\text{rough}} = \left[1 + 0.42\,\frac{\text{Re}_{\Delta x}}{\text{Re}_{w1}^{1.25}\,(1+K_1)^{1.25}}\right]^{-0.8} = [1 + 0.42R]^{-0.8} \tag{6}$$

valid at $\text{Re} \geqslant \text{Re}_{\text{cr}2}$.

The efficiency of a gaseous shield was studied experimentally in an apparatus consisting essentially of a closed-type wind tunnel with an open test segment. This apparatus is shown schematically in Fig. 3. A regulation system facilitated smooth variation of the stream velocity from 10 to 40 m/sec and ensured its maintenance at any constant level within this range. The tunnel had been constructed so as to make it possible to attain uniform velocity distributions over cross sections throughout the entire length of its open test segment. The steam turbulence level did not exceed 2%.

The experimental part was a flat plate placed horizontally at the center of the test segment, along the axis of the air stream. This plate consisted of a preengaged permeable segment 15 with the dimensions 200 × 178 × 20 mm, a thermally insulated segment 16, and two splitters. The porous walls were made of permeable mesh material according to a technology developed at the N. E. Bauman Moscow Higher Technical School. Into the porous walls were inserted and sealed nine Chromel–Copel thermocouples made of wire 0.2 mm in diameter for measuring the surface temperature, and inside a basket underneath the porous plates were placed two thermocouples for measuring the temperature of the injected air.

The thermally insulated segment of the plate was made of two 10-mm-thick Textolite strips joined together tightly along their lateral surfaces. For measuring the wall temperature on both sides, into the plate were sealed 18 Chromel–Copel thermocouples of wire 0.2 mm in diameter. For insertion of these thermocouples, holes 1 mm in diameter had been drilled into the plate on both the right side and the left side of its center line. These holes on both sides of the Textolite had been connected by grooves, into which the thermocouple leads were laid. The thermocouples were installed with their leads on the center line of the plate, so as to minimize the error of temperature readings due to heat leakage along the thermocouple wires.

Roughness on one side of the plate was produced by laying on top of it a structure, with the appropriate asperity profile, made of Micarta. The 0.2-mm wires of Chromel–Copel thermocouples were sealed flush to the profile structure at the tips of its asperities. The

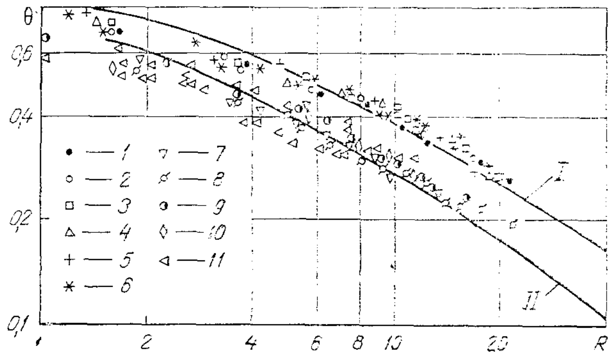

Fig. 4. Comparison of measured and calculated efficiencies of gaseous shield: I) calculation according to expression (2); II) calculation according to expression (6). Experiment with smooth plate: 1) j = 0.089, 2) j = 0.087, 3) j = 0.008., 4) j = 0.011, 5) j = 0.01, 6) j = 0.012; experiment with rough plate: 7) j = 0.012, 8) j = 0.011, 9) j = 0.01, 10) j = 0.084; 11) measurements [6].

air injection system for producing a gaseous shield consisted of an electric compressor 1, a battery of high-pressure air tanks, an air preheater 11, and flow measuring washers 10. The helical air preheater had been designed for raising the air temperature to 140°C.

The following parameters were measured during the experiment:

surface temperatures of the porous wall, the smooth wall, and the thermally insulated rough wall;

temperature and flow rate of injected air; and

velocity and temperature profiles in the boundary layer above the surface of the experimental plate piece.

For temperature measurements a special-purpose automatic complex 12 was used, consisting of a programmable automatic device with control modules, a digital voltmeter, and a recording photographic camera. Up to 51 thermocouples could be simultaneously connected to this measuring complex.

Velocity and temperature profiles in the boundary layer were measured with a compound probe 17. As velocity gauge served A Pitot tube, made of an injection needle with a 1 × 0.2 mm large inlet orifice, a static-pressure tube 0.8 mm in diameter with pointed tip, and a hole 0.5 mm in diameter drilled into it at a distance of 15 mm from the tip, served as a velocity gauge. The velocity head was measured with a type MMN manometer with oblique scale. Temperature profiles were measured with a Chromel—Copel thermocouple made of wire 0.1 mm in diameter.

Tests were performed with the velocity of the stream core varied from 12 to 35 m/sec and the intensity of injection through the permeable segment varied over the j = 0.0077-0.012 range. Semicylinders 16 mm in diameter served as asperities, making the surface rough. The relative pitch between asperities was varied from 2 to 6.

Preliminary measurements on a smooth surface without air injection through the permeable segment have revealed a turbulent boundary layer with the usual power-law velocity profile $\omega_0 = (y/\delta)^{1/7}$ developing over almost the entire plate, and a gaseous shield forming on the smooth wall (Fig. 4) with an efficiency described accurately enough by expression (2), as verified by the numerous experimental data of several other authors [1].

The experimental efficiency of a gaseous shield was determined in two ways:

1) Directly from temperature readings taken at the thermally insulated segment (T_W), at the end of the permeable segment (T_{W1}), and in the stream (T_0):

$$\theta = \frac{T_W - T_0}{T_{W1} - T_0};$$

2) from the law of energy conservation in the boundary layer above the thermally insulated segment [1]

$$\theta = \frac{\delta_{T1}^{**}}{\delta_T^{**}},$$

with $\delta_{T_1}^{**}$ and δ_T^{**} denoting the energy thickness of the boundary layer above the permeable segment and in a given section above the thermally insulated plate, respectively, both determined through graphical integration with the aid of measured velocity and temperature profiles in the boundary layer of air

$$\delta_T^{**} = \int_0^\delta \frac{\rho u}{\rho_0 u_0} \frac{T - T_0}{T_W - T_0} dy.$$

The difference between values of efficiency obtained by these two methods did not exceed 5%.

The results of efficiency measurements performed on a gaseous shield over the rough surfaces in this study are shown in Fig. 4. The intensity of injection through the preengaged porous segment was varied over the 0.084-0.012 range.

In all cases the rough surface was streamlined at $Re > Re_{cr2}$ and the measured velocity profiles above surface asperities were described accurately enough by expression (4), as shown in Fig. 2. The efficiency of a gaseous shield measured at surface asperities did not depend on the spacing of the latter, within the given range of their relative pitch.

The graph in Fig. 4 indicates that the proposed relation (6) does sufficiently accurately generalize the experimental data of this study and other readings [6], obtained under conditions of square-law drag of the rough surface.

NOTATION

θ is the efficiency of a gaseous shield on a smooth surface; θ_{rough}, efficiency of a gaseous shield on a rough surface; T_W, temperature of the thermally insulated wall, °K; T_0, temperature of the air stream, °K; $\psi_{rough} = c_{f,rough}/c_{f0}$, law of friction at the rough surface; $c_{f,rough}$, friction coefficient at a rough wall; c_{f0}, friction coefficient at a smooth wall; T_{W1}, temperature at the end of the permeable segment, °K; $Re_{\Delta x} = \frac{\rho_0 u_0 (x - x_1)}{\mu}$ and $Re_{W1} = j_{W1} x_1/\mu$, Reynolds numbers; x_1, length of the permeable segment, m; j_W, mass rate of air injection, kg/m·sec; δ, thickness of the boundary layers; δ^{**}, momentum thickness, m; δ^*, displacement thickness, m; δ_T^{**}, thickness of energy loss, m; $K_1 = (T' - T_{W1})/(T_{W1} - T_0)$, temperature coefficient accounting for heat transfer at the permeable segment; T', temperature of injected air, °K; and $\omega = u/u_0$, relative velocity.

LITERATURE CITED

1. S. S. Kutateladze and A. I. Leont'ev, Heat Transfer and Friction in Turbulent Boundary Layer [in Russian], Energiya, Moscow (1972).
2. Goldstein, Shavit, and Chen, "Efficiency of film cooling with injection through porous wall," Heat Transfer, No. 3, 36-46 (1965).
3. V. P. Komarov and A. I. Leont'ev, "Experimental study of efficiency of shield in turbulent boundary layer of gas," Teplofiz. Vys. Temp., No. 2, 353-358 (1970).
4. É. P. Volchkov, "Turbulent boundary layer under conditions of gaseous shield and chemical reactions on surface," Author's Abstract of Doctoral Dissertation, Technical Sciences, Novosibirsk (1972).
5. V. K. Koz'menko, "Experimental study of gaseous shield in nozzles with various modes of flow," Author's Abstract of Candidate's Dissertation, Technical Sciences, Novosibirsk (1980).
6. É. P. Volchkov and V. Ya. Levchenko, "Efficiency of gaseous shield on tubular surface," Zh. Prikl. Mekh. Tekh. Fiz., No. 1, 115-120 (1966).
7. É. P. Volchkov and V. Ya. Levchenko, "Heat transfer at protective jet shield on surfaces," Zh. Prikl. Mekh. Tekh. Fiz., No. 2, 135-137 (1966).
8. Herman and Kestin Schlichting, Boundy Layer Theory, McGraw (1968).
9. Townes, Howe, Pauh, and Weber, "Turbulent flow through smooth and rough pipes," Theor. Principles Eng. Calc., No. 2, 108-119 (1972).

10. L. L. Kobzar', "Hydrodynamic characteristics of turbulent flow through smooth and rough pipes," Author's Abstract of Candidate's Dissertation, Technical Sciences, Obninsk (1973).
11. Antonia and Luxton, "Response of turbulent boundary layer to step change in surface roughness," J. Fluid Mech., 48, Part 4, 721-761 (1971).
12. Perry, Schofield, and Joubert, "Rough-wall turbulent boundary layers," J. Fluid Mech., 37, Part 2, 383-413 (1969).
13. Moffat, Hilser, and Keyes, "Experimental study of heat transfer in turbulent boundary layer at rough surface with injection," Heat Transfer, No. 1, 145-155 (1978).
14. B. M. Teverovskii, "Effect of surface roughness on hydraulic drag and convective heat transfer," Izv. Vyssh. Uchebn. Zaved., Energetika, No. 7, 84-89 (1958).
15. N. M. Galin, "Heat transfer during turbulent flow of fluids at rough walls," Author's Abstract of Candidate's Dissertation, Technical Sciences, Moscow (1966).

DRAG OF CRISSCROSS BUNDLES OF FINNED TUBES IN TRANSVERSE STREAM OF FLUID

A. A. Zhukauskas, R. V. Ulinskas, and F. V. Zinyavichyus

UDC 536.24

Experimental data are presented on the form resistance and the hydraulic drag of crisscross bundles of finned tubes, whereupon the Berman number and the Chen number are calculated for the near zone of the wake behind a finned tube.

In modern power engineering equipment one often uses heat exchangers with finned heating surfaces.

A survey of published studies reveals that no basic research has been done on bundles of finned tubes in a transverse air stream and that no detail data are available on the heat transfer at such bundles and their drag in a stream of viscous fluid.

In one study [1], the pressure distribution was determined around a tube with three different types of transverse finning, in the fourth row of a 1.64 × 1.42 crisscross bundle at $Re = 2.93 \cdot 10^4$ and at $Re = 3.01 \cdot 10^4$; in another study [2], such tubes, all with the same type of finning, were used in each row of a 1.93 × 1.69 crisscross bundle and in a 1.93 × 1.87 corridor bundle for determination of the pressure distribution at $Re = 3.1 \cdot 10^4$.

The experimental data obtained by various authors pertaining to hydraulic drag of bundles of tubes have been subsequently generalized [3, 4].

The objects of this study were eight crisscross bundles in various configurations, with the effective tube finning parameter h/s varied over approximately the 0.3-1.6 range. Typical data have been obtained on the local hydrodynamic characteristics of compact finned tube bundles, much attention now being devoted to the study of such bundles. In these studies one simultaneously determines the optimum geometrical characteristics for heat transfer and for streamlining by high-viscosity fluids, with the Prandtl number varying from 80 to 5000 and the Reynolds number varying from 20 to $2 \cdot 10^6$.

Method of Study. The study was made using a circulation system with transformer oil [5].

The dependence of the drag on the tube finning parameters was studied with tubes in a bundle spaced longitudinally and transversely in uniform steps (bundles No. 6-8 in Table 1). An "infinite" bundle was composed of half-tubes. The experimental tubes (Fig. 1), furnished with pressure-head gauges, had the following dimensions: L = 150, β - 2-4°, and d, h, δ_1, δ_2 either 45, 15, 1.29, 9 or 15, 5, 0.43, 3, respectively.

Institute of Physicotechnical Problems in Power Engineering, Academy of Sciences of Lithuanian SSR, Kaunas. Translated from Inzhenerno-Fizicheskii Zhurnal, Vol. 43, No. 6, pp. 891-898, December, 1982. Original article submitted November 30, 1981.

 0022-0841/82/4306-1314$07.50